

Quasiperiodic perturbations of Stokes waves: Secondary bifurcations and stability

Sergey A. Dyachenko¹ and Anastassiya Semenova²

¹ *Department of Mathematics, SUNY at Buffalo, Buffalo, NY, USA*

² *Department of Applied Mathematics, University of Washington, Seattle, WA, USA*

Abstract

We develop a numerical method based on canonical conformal variables to study two eigenvalue problems for operators fundamental to finding a Stokes wave and its stability in a 2D ideal fluid with a free surface in infinite depth. We determine the spectrum of the linearization operator of the quasiperiodic Babenko equation, and provide new results for eigenvalues and eigenvectors near the limiting Stokes wave identifying new bifurcation points via the Fourier-Floquet-Hill (FFH) method. We conjecture that infinitely many secondary bifurcation points exist as the limiting Stokes wave is approached. The eigenvalue problem for stability of Stokes waves is also considered. The new technique is extended to allow finding of quasiperiodic eigenfunctions by introduction of FFH approach to the canonical conformal variables based method. Our findings agree and extend existing results for the Benjamin-Feir, high-frequency and localized instabilities. For both problems the numerical methods are based on Krylov subspaces and do not require forming of operator matrices. Application of each operator is pseudospectral employing the fast Fourier transform (FFT), thus enjoying the benefits of spectral accuracy and $O(N \log N)$ numerical complexity. Extension to nonuniform grid spacing is possible via introducing auxiliary conformal maps.

1 Introduction

Waves on the surface of the ocean appear due to multiple sources ranging from large scales such as seismic disturbances, motion of celestial bodies to the small scales dominated by forces of surface tension and dissipation. Ocean and atmosphere are intertwined systems, and wind is one of the primary forces responsible for wave generation. The details of generation of water waves by wind remain elusive, and it is generally thought to be a combination of the Miles-Phillips mechanism [1, 2] together with ideas of Jeffreys' sheltering theory [3]. Nevertheless, ocean surface can be decoupled from atmospheric effects when long ocean waves are considered. As waves travel away from an epicenter of a storm, the long waves can be viewed as almost unidirectional periodic waves.

Traveling waves propagating at a fixed speed without changing shape are called the Stokes waves. They are special solutions of 2D Euler equations originally discovered by Stokes in [4, 5] and later studied in many works [6, 7, 8, 9, 10, 11, 12, 13, 14, 15].

The Stokes waves are a one-parameter family of solutions, and steepness is commonly used for parameterization. It is denoted by $s = H/\Lambda$, and is defined as the ratio of crest-to-trough height H , over the wavelength Λ . The steepness ranges from zero to $s_{lim} = 0.14106348398\dots$ (see also Refs. [16, 17, 18, 19, 20]) in the limiting Stokes wave, or the wave of greatest height, which forms an angular crest with 120° . Existence of such limiting wave has been proven in the works of [21, 22, 23].

The primary branch of Stokes waves contains solutions having one wavecrest per period. A secondary (double-period) bifurcation from the primary branch leads to a different branch of solutions having double the period of the original Stokes wave [24, 25, 26, 27]. Each period contains a pair of wavecrests that are distinct. Similarly, the secondary bifurcations happen for other ratios relative to primary period (e.g. tripling), and such bifurcations are effectively handled via the Floquet theory.

Dynamics of Stokes waves can be studied in the framework of Euler equations. The Hamiltonian framework to study the time-evolution of potential flow of an ideal fluid with free surface has been established in [28]. Equations governing the motion of a fluid surface in conformal variables were derived in [29, 30, 31, 32, 33], and wave breaking was numerically explored in [34, 35]. Instabilities of Stokes wave have been studied in many works [36, 37, 38, 39, 28, 40, 41, 42, 43] including numerical studies [44, 45, 46, 47]. Stokes waves are unstable to long wave perturbations, a.k.a the *subharmonic* perturbations, such as the Benjamin-Feir (BF) or modulational instability, first reported in [36, 48, 39] and high-frequency instability [44, 49, 50, 42]. Recent theoretical studies of Benjamin-Feir instability for small amplitude waves are described in [49, 41, 43]. The *superharmonic* instability corresponds to growth of co-periodic perturbations and has been described in [51] and found numerically in [52, 53] with almost limiting waves considered in [46, 54, 47].

In the present work, we consider two eigenvalue problems connected to Stokes waves. In the first problem (see Section 6), we developed a numerical method that is based on Krylov subspaces to find eigenvalues and eigenfunctions of the linearized Babenko equation [55]. It is spectrally accurate, matrix-free and has $O(N \log N)$ numerical complexity, where N is the number of Fourier modes approximating a Stokes wave. We extend the method with FFH approach [56] to study quasiperiodic eigenfunctions. Appearance of additional zero eigenvalue is found to occur at either a turning point of speed, or at a secondary bifurcation from the primary branch of Stokes waves. We report new secondary bifurcations (see also [27]) and conjecture that infinite number of bifurcations may occur as the limiting Stokes wave is approached. Novel results are found for eigenfunctions of the linearized Babenko equation, and qualitative similarity with the classical Sturm-Louisville problem is observed. The eigenfunctions become strongly concentrated near the wavecrest, and may be related to the structure of the transition layer around the wavecrest [20]. The linearized Babenko operator is self-adjoint, and thus the set of its eigenfunctions is complete. The eigenfunctions of Babenko equation may be significant for theoretical study of wave-breaking phenomena similar to [57, 58] to describe numerical observations in Refs. [35, 47].

In the second problem (see Section 7) we seek eigenvalues and eigenfunctions for the equations of motion linearized around the Stokes wave. We extended the canonical conformal variables based method (CCVM) in [59] with the Fourier-Floquet-Hill approach to study stability of Stokes waves to quasiperiodic disturbances. It is shown how a quadratic eigenvalue problem (QEP) with a pair of self-adjoint, and a skew-adjoint

operators can be obtained. The QEP is solved efficiently via Krylov subspace based method avoiding matrix formation, having spectral accuracy and $O(N \log N)$ complexity. We provide examples that confirm and extend the stability results for superharmonic instabilities that were found by linearization in Tanveer-Dyachenko variables [54], and provide new results for Benjamin-Feir, high-frequency and localized instabilities of Stokes waves. Additional results obtained by the present method are reported in the work [47].

2 Euler equations with free surface

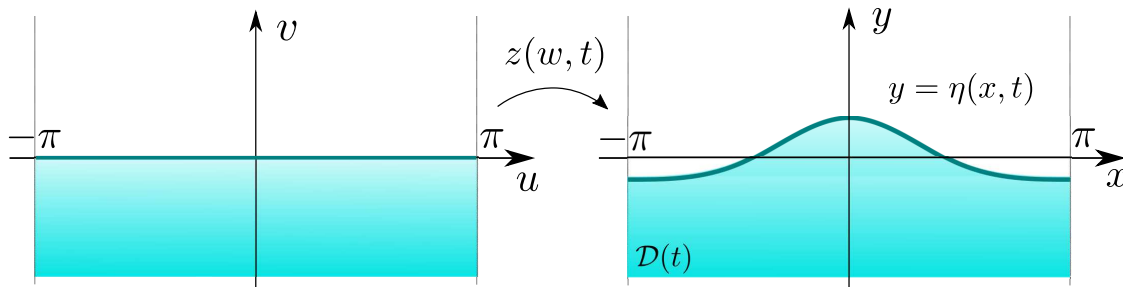


Figure 1: The time-dependent conformal transformation $z(w, t) = x(w, t) + iy(w, t)$ maps 2π -periodic semi-infinite strip in $w = u + iv$ -plane (left panel) to 2π -periodic infinitely deep fluid domain $\mathcal{D}(t)$ (right panel). The line $v = 0$ is mapped to the free surface $y = \eta(x, t)$.

We consider a potential flow of an ideal fluid of infinite depth with a free surface at $z = x + i\eta(x, t)$ (see Fig. 1). The fluid velocity is given by $\mathbf{v} = \nabla\varphi$ where $\varphi(x, y, t)$ is the velocity potential and $\nabla = (\partial_x, \partial_y)^T$. By virtue of incompressibility φ satisfies the Laplace equation $\Delta\varphi = 0$ in the fluid domain $\mathcal{D}(t)$ and the following boundary conditions are imposed at the free surface $y = \eta(x, t)$ and at the bottom of the fluid domain,

$$\frac{\partial\eta}{\partial t} + \left(\frac{\partial\eta}{\partial x} \frac{\partial\varphi}{\partial x} - \frac{\partial\varphi}{\partial y} \right) \Big|_{y=\eta(x,t)} = 0 \quad (1)$$

$$\left(\frac{\partial\varphi}{\partial t} + \frac{1}{2} (\nabla\varphi)^2 \right) \Big|_{y=\eta(x,t)} + g\eta = 0 \quad (2)$$

$$\frac{\partial\varphi}{\partial y} \Big|_{y \rightarrow -\infty} = 0 \quad (3)$$

where g is gravity acceleration. We introduce the surface potential, $\psi(x, t) = \varphi(x, \eta(x, t), t)$, and the variables $\psi(x, t)$ and $\eta(x, t)$ are the canonical variables as shown in [28].

2.1 Hamiltonian and conformal variables

The system (1)–(3) together with Laplace equation is described by methods of Hamiltonian mechanics. The Hamiltonian is given by,

$$\mathcal{H} = \frac{1}{2} \int_{-\pi}^{\pi} \int_{-\infty}^{\eta(x,t)} (\nabla\varphi)^2 dx dy + \frac{g}{2} \int_{-\pi}^{\pi} \eta^2 dx, \quad (4)$$

which is the sum of kinetic and potential energy of the fluid. Following the work [60], we express Hamiltonian as surface integrals as follows:

$$\mathcal{H} = \frac{1}{2} \int_{-\pi}^{\pi} \psi \frac{\partial\varphi}{\partial\mathbf{n}} \Big|_{y=\eta(x,t)} dx + \frac{g}{2} \int_{-\pi}^{\pi} \eta^2 dx, \quad (5)$$

where \mathbf{n} is the normal to the free surface, and Dirichlet-to-Neumann operator must be introduced to express the normal derivative of the potential at the free surface through ψ and η . The variables ψ and η are the canonical momentum and coordinate in physical variables, and the system:

$$\frac{\partial\eta}{\partial t} = \frac{\delta\mathcal{H}}{\delta\psi}, \quad \frac{\partial\psi}{\partial t} = -\frac{\delta\mathcal{H}}{\delta\eta}, \quad (6)$$

is equivalent to the system (1)–(3). Instead of writing the Hamiltonian in the the variables ψ, η we follow [60] and introduce a conformal mapping from $w = u + iv \in \mathbb{C}^-$ to $\mathcal{D}(t)$ denoted by $z(w, t) = x(w, t) + iy(w, t)$ (see Fig. 1). In conformal variables, the free surface is described in parametric form,

$$z(u, t) = x(u, t) + iy(u, t) = u - \hat{H}y(u, t) + iy(u, t), \quad (7)$$

where \hat{H} is the circular Hilbert transform defined as $\hat{H}e^{iku} = i \text{sign}(k)e^{iku}$.

We abuse notation to define, $\psi(u, t) := \varphi(x(u, t), y(u, t), t)$ and $y(u, t) := \eta(x(u, t), t)$. The Hamiltonian in the conformal variables can be written explicitly as follows,

$$\mathcal{H} = \frac{1}{2} \int_{-\pi}^{\pi} \psi \hat{k} \psi du + \frac{g}{2} \int_{-\pi}^{\pi} y^2 x_u du, \quad (8)$$

with $\hat{k} = -\partial_u \hat{H}$, hence the Fourier symbol for \hat{k} is $|k|$. The Lagrangian in the conformal variables is given by,

$$\mathcal{L} = \int \psi \eta_t dx - \mathcal{H} = \int \psi (y_t x_u - y_u x_t) du - \mathcal{H}, \quad (9)$$

$$\mathcal{L} = \int (x_u \psi - \hat{H}[y_u \psi]) y_t du - \mathcal{H}, \quad (10)$$

and canonical conformal momentum $\mathcal{P} := x_u \psi - \hat{H}[y_u \psi] =: \hat{\Omega}_{21}^\dagger \psi$ is introduced as in [61], and write:

$$\mathcal{L} = \int \mathcal{P} y_t du - \mathcal{H}(\mathcal{P}, y), \quad \mathcal{H} = \frac{1}{2} \int \mathcal{P} \hat{R}_{12} \hat{k} \hat{R}_{12}^\dagger \mathcal{P} du + \frac{g}{2} \int y^2 x_u du, \quad (11)$$

with $\psi = \frac{x_u \mathcal{P} + \hat{H}[y_u \mathcal{P}]}{|z_u|^2} =: \hat{R}_{12}^\dagger \mathcal{P}$. Here the definitions of operators $\hat{\Omega}_{21}$ and \hat{R}_{12} are in agreement with [62] and $\hat{R}_{12} \hat{\Omega}_{21} = 1$, with dagger denoting the adjoint operator. In the variables \mathcal{P} and y , the system acquires canonical structure,

$$\frac{\partial y}{\partial t} = \frac{\delta H}{\delta \mathcal{P}}, \quad \frac{\partial \mathcal{P}}{\partial t} = -\frac{\delta H}{\delta y}. \quad (12)$$

The canonical variables \mathcal{P} and y naturally appear in numerical method for stability problem which is described in the Section 7.

3 Implicit form and Babenko equation

Equations of motion in implicit form are determined from the stationary action principle with Lagrangian defined in (9),

$$\mathcal{S} = \int (\mathcal{L} + \mathcal{C}) dt, \quad (13)$$

$$\mathcal{C} = \int f(y - \hat{H}[x - u]) du, \quad (14)$$

where \mathcal{S} is action, \mathcal{C} is a Lagrangian constraint, and f is the Lagrange multiplier ensuring that x and y are related by the Hilbert transform. The equations of motion are obtained from extremizing action which implies that,

$$\frac{\delta \mathcal{S}}{\delta x} = 0, \quad \frac{\delta \mathcal{S}}{\delta y} = 0, \quad \frac{\delta \mathcal{S}}{\delta \psi} = 0 \quad \text{and} \quad \frac{\delta \mathcal{S}}{\delta f} = 0 \quad (15)$$

and solving for the Lagrange multiplier f (see also Ref. [60]) yields,

$$y_t x_u - y_u x_t = -\hat{H} \psi_u, \quad (16)$$

$$\psi_t x_u - x_t \psi_u + \hat{H} [-y_u \psi_t + y_t \psi_u] + g [y x_u - \hat{H}(y y_u)] = 0. \quad (17)$$

We switch to the reference frame traveling with the speed of a Stokes wave by considering the following ansatz,

$$y(u, t) \rightarrow y(u - ct, t), \quad \text{and} \quad x(u, t) \rightarrow u - \hat{H} y(u - ct, t), \quad (18)$$

$$\psi(u, t) \rightarrow \phi(u - ct, t) - c \hat{H} y(u - ct, t), \quad (19)$$

where c is the velocity of the moving frame.

Substitution of (18)-(19) into the equations of motion (16)-(17) leads to the following system in the moving reference frame:

$$x_u y_t - y_u x_t = -\hat{H} (\phi_u - c), \quad (20)$$

$$x_u \phi_t - x_t \phi_u - \hat{H} [y_u \phi_t - y_t \phi_u] + 2c x_t = c^2 \hat{k} y - g (x_u y - \hat{H} [y y_u]). \quad (21)$$

The Stokes wave is a stationary solution of the latter system. It is found by setting $x_t = y_t = \phi_t = 0$ in(20)-(21) which leads to the relations:

$$\phi_u = 0, \quad \text{or} \quad \psi_u = c(x_u - 1) = -c \hat{H} y_u = c \hat{k} y, \quad (22)$$

$$\hat{S} y := c^2 \hat{k} y - g [x_u y - \hat{H} (y y_u)] = 0. \quad (23)$$

The latter equation is also sometimes referred to as the Babenko equation [55]. The operator $\hat{S}_1(y)$ is linearized around a Stokes wave $y(u)$ to form $\hat{S}_1(y)\delta y$ as follows,

$$\hat{S}_1(y)\delta y := \left(c^2\hat{k} - g\right) \delta y - g \left[y\hat{k}\delta y + \delta y\hat{k}y + \hat{k}(y\delta y)\right] \quad (24)$$

which is *hermitian*, i.e. $\hat{S}_1^\dagger = \hat{S}_1$ with standard inner product.

The discussion of eigenvalue problem for \hat{S}_1 , its significance as well as new results and the numerical method is presented in the Section 6 of this paper.

4 Linearization of the implicit equations of motion

Linear stability is determined by the eigenvalue spectrum of linearization operator of the system (20)–(21) around a Stokes wave, $y(u)$. After substitution of the ansatz, $y(u, t) \rightarrow y(u) + \delta y(u, t)$ and $\phi(u, t) \rightarrow 0 + \delta\phi(u, t)$ in (20)–(21) and keeping only the linear terms in δy and $\delta\phi$ we obtain the linearized equations of motion,

$$x_u\delta\phi_t - \hat{H}[y_u\delta\phi_t] - 2c\hat{H}\delta y_t = \hat{S}_1(y)\delta y, \quad (25)$$

$$x_u\delta y_t + y_u\hat{H}\delta y_t = -\hat{H}\delta\phi_u. \quad (26)$$

The equations (25)–(26) are convenient to express in the operator matrix form:

$$\hat{L} \begin{bmatrix} \delta\phi_t \\ \delta y_t \end{bmatrix} = \hat{M} \begin{bmatrix} \delta\phi \\ \delta y \end{bmatrix}, \quad (27)$$

with the following operator matrices:

$$\hat{M} = \left[\begin{array}{c|c} \hat{k} & 0 \\ \hline 0 & \hat{S}_1 \end{array} \right], \quad \hat{L} = \left[\begin{array}{c|c} 0 & \hat{\Omega}_{21} \\ \hline \hat{\Omega}_{21}^\dagger & -2c\hat{H} \end{array} \right]. \quad (28)$$

Equivalently, the first-order system (27) given by

$$\hat{\Omega}_{21}^\dagger\delta\phi_t - 2c\hat{H}\delta y_t - \hat{S}_1\delta y = 0, \quad (29)$$

$$\hat{\Omega}_{21}\delta y_t = \hat{k}\delta\phi \quad (30)$$

is expressed as a second order equation by solving (30) for $\delta\phi$ and substituting the result into (29),

$$\hat{\Omega}_{21}^\dagger\hat{k}^{-1}\hat{\Omega}_{21}\delta y_{tt} - 2c\hat{H}\delta y_t - \hat{S}_1\delta y = 0. \quad (31)$$

The equation (31) leads to a quadratic eigenvalue problem (QEP) with substitution $\partial_t \rightarrow \lambda$ which determines the stability of Stokes waves.

4.1 Dispersion of linear gravity waves

The linear waves are stable, and the dispersion relation of linear waves in laboratory frame is given by:

$$\omega(k) = \pm\sqrt{g|k|}. \quad (32)$$

This relation is trivially found from the QEP by noting that for a flat surface:

$$\hat{\Omega}_{21} = \hat{\Omega}_{21}^\dagger = 1, \quad (33)$$

$$\hat{S}_1 = c^2 \hat{k} - g. \quad (34)$$

Then, the substitution of the plane wave in the form $\delta y \sim e^{i(ku - \omega t)}$ leads to

$$\omega(k) = ck \pm \sqrt{g|k|}, \quad (35)$$

where the term ck is a Doppler frequency shift from moving to the traveling frame of reference.

We discuss the details of the numerical method for the system (29)–(30) and new results obtained for the stability problem of large amplitude waves in the section 7.

5 Fourier-Floquet-Hill method in conformal variables

In order to consider quasiperiodic eigenfunctions we use the Fourier-Floquet-Hill method (FFH) described in [56] and implemented in [44, 46]. We seek quasiperiodic eigenfunctions $f(u)$ described by the trigonometric series:

$$f(u) = \tilde{f}(u)e^{i\mu u} = \sum_{k=-\infty}^{\infty} \tilde{f}_k e^{i(k+\mu)u}, \quad (36)$$

where $\tilde{f}(u)$ is a 2π -periodic function. We consider the operators of linearized equations of motion when applied to a quasiperiodic function f ,

$$\hat{k}f = \hat{k} \left(\sum_{k=-\infty}^{\infty} \tilde{f}_k e^{i(k+\mu)u} \right) = e^{i\mu u} \sum_{k=-\infty}^{\infty} |k + \mu| \tilde{f}_k e^{iku} = e^{i\mu u} \hat{k}_\mu \tilde{f}. \quad (37)$$

Hence, the operator \hat{k} acts as multiplier $|k + \mu|$ in the Fourier space. The linearized Babenko operator applied to f is given by,

$$\hat{S}_1 f = e^{i\mu u} S_{1,\mu} \tilde{f} = e^{i\mu u} \left[(c^2 \hat{k}_\mu - g) \tilde{f} - g (y \hat{k}_\mu \tilde{f} + \tilde{f} \hat{k}_\mu y + \hat{k}_\mu (y \tilde{f})) \right], \quad (38)$$

and finally:

$$\hat{\Omega}_{21} f = x_u f + y_u \hat{H} f = e^{i\mu u} \left[x_u \tilde{f} + y_u \hat{H}_\mu \tilde{f} \right] = e^{i\mu u} \hat{\Omega}_{21,\mu} \tilde{f}, \quad (39)$$

$$\hat{\Omega}_{21}^\dagger f = x_u f - \hat{H} (y_u f) = e^{i\mu u} \left[x_u \tilde{f} - \hat{H}_\mu (y_u \tilde{f}) \right] = e^{i\mu u} \hat{\Omega}_{21,\mu}^\dagger \tilde{f}, \quad (40)$$

where $\hat{H}_{k,\mu} = i \operatorname{sign}(k + \mu)$ is the Fourier multiplier for the quasiperiodic Hilbert transform, \hat{H}_μ .

6 Results: Eigenvalues of \hat{S}_1 .

Occurrence of zero eigenvalues in \hat{S}_1 (aside from the trivial zero associated with Galilean invariance) indicates appearance of extra eigenfunction in the null space of \hat{S}_1 and corresponds to a turning point of speed, or a secondary bifurcation from a branch of Stokes waves. We study the eigenvalues Since \hat{S}_1 is self-adjoint its eigenvalues are real, and linearization at a flat surface indicates that Fourier modes are the eigenfunctions as evident from,

$$\hat{S}_1 f \rightarrow (c^2 \hat{k} - g) f. \quad (41)$$

Hence the eigenvalues are the integers $\xi = -1, 0, 1, \dots$ (with $c = 1$ and $g = 1$). Each eigenvalue except -1 has multiplicity 2. The double eigenvalue 0 (for $s = 0$) signifies a primary bifurcation from the flat surface to a nonlinear Stokes wave (see Fig. 2). In case of a flat surface $\xi_k = |k - 1|$ is an eigenvalue for $k = 0, 1, \dots$. Each eigenvalue except $\xi_0 = -1$ has a 2-dimensional eigenspace spanned by the functions $e^{\pm iku}$, or equivalently $\cos ku$ and $\sin ku$, associated with ξ_k .

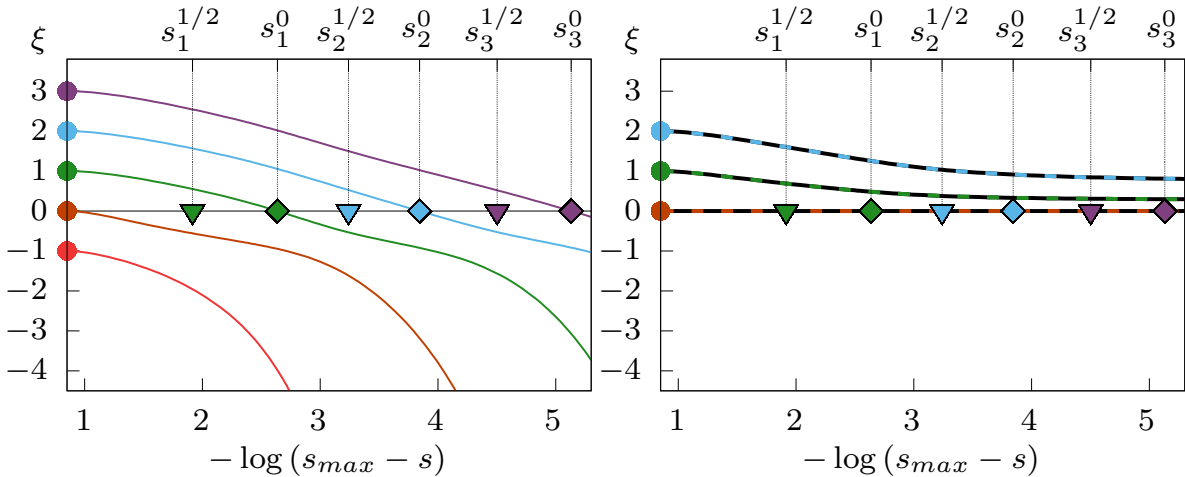


Figure 2: The first few eigenvalues ξ of \hat{S}_1 as a function of the Stokes wave steepness. At flat surface each eigenvalue has multiplicity 2 (orange, green, blue and violet circles), except -1 which is simple (red circle). The double eigenvalues break into simple eigenvalues in finite amplitude Stokes waves. (Left Panel) The eigenvalues originating from a flat surface at $\xi = -1, 0, 1, 2, 3$ are colored in red, orange, green, blue and violet respectively; and (Right Panel) the second eigenvalue originating from $\xi = 0, 1, 2$ are marked dashed red, dashed green and dashed blue respectively. The green, blue and violet diamonds correspond to bifurcation points at the turning points of speed, and the triangles denote the double-period bifurcations.

Away from the flat surface, the eigenvalues of operator \hat{S}_1 are found numerically. Each eigenvalue becomes simple, except for the special cases when collisions of eigenvalues occur. A pair of eigenvalues originating from a double eigenvalue in a flat surface follow distinct paths: one eigenvalue corresponding to an even eigenfunction crosses the zero axis, whereas the other one remains positive. The Fig. 2 illustrates typical behaviour of eigenvalues associated with even and odd eigenfunctions as a function of steepness.

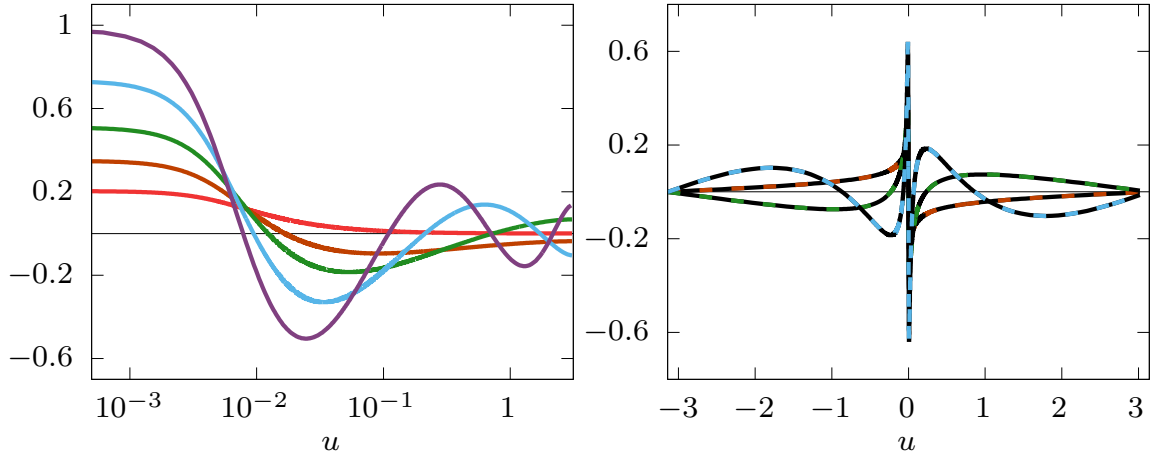


Figure 3: (Left Panel) The first five even eigenfunctions associated with eigenvalues at $s = 0.1388325$ (same colormap as in the left panel Fig. 2), and (Right Panel) the first three odd eigenfunctions corresponding to the eigenvalues of the right panel of Fig. 2.

For *regular waves*, the linearization operator \hat{S}_1 has a simple zero eigenvalue and associated eigenfunction y_u :

$$\hat{S}_1 y_u = \partial_u (\hat{S} y) = 0, \quad (42)$$

and corresponds to translational invariance of solutions to Babenko equation.

At the bifurcation points (see Fig. 2) the zero eigenvalues has double multiplicity, and the additional eigenpair is associated with either the turning points in the $c(s)$ graph, or the secondary bifurcations from the primary branch (when subharmonics are considered). See also the table 1 in the section 6.1 for the few first secondary bifurcations and turning points.

The Fig. 2 illustrates the dependence of the first few eigenvalues ξ_j of \hat{S}_1 on steepness, s . All the eigenvalues we found do not increase with steepness, i.e. $\partial_s \xi_j \leq 0$ for all j . Eventually half of eigenvalues cross the horizontal axis at turning points of speed at $s = s_1^0, s_2^0, \dots$ and become negative. Since the number of eigenvalues is infinite, it is conjectured that zero eigenvalue appears infinitely many times as the extreme wave is approached, and is in agreement with [12]. Tracking the eigenvalues crossing the origin, one may find secondary bifurcations corresponding to appearance of irregular waves discovered in [24] and for finite depth in [63]. In such case, the eigenvalue problem comes from linearization around two periods of a Stokes wave.

Fig. 3 shows the first few eigenfunctions for a large amplitude wave with steepness $s = 0.1388325$. In the case of a flat surface the even eigenfunctions are given by

$$f_1(u) = 1, \quad f_2(u) = \cos u, \quad f_3(u) = \cos 2u, \quad \dots \quad (43)$$

The eigenfunctions continuously deform as we follow the primary branch and approach the limiting wave. Odd eigenfunctions continuously deform from $\sin(ku)$, but the corresponding eigenvalues never cross zero.

In addition we find that as the limiting wave is approached, the eigenfunctions become concentrated near the wave crest (see the Fig. 3) suggesting self-similar behaviour of the boundary layer near wave-crest discussed in [16, 20]. In the remainder of the

interval the eigenfunctions look qualitatively similar to the Fourier cosine/sine of the appropriate wavenumber.

6.1 Bifurcation points of the linearized Babenko equation

In this section we demonstrate several waves at bifurcations associated with turning points of speed ($\mu = 0$ coperiodic) and double period bifurcations ($\mu = 1/2$) in the primary branch. The result for double-period bifurcation point at $s_1^{\mu=1/2}$ has been determined in [24, 64], see also [25] for more bifurcation points corresponding to tripling and higher wavelength multiples. We report a new bifurcation point at $s_3^{\mu=1/2} = 0.141032049$ located between the first minimum and the second maximum of the Stokes wave speed.

Notation	Steepness, s	Description
	0	primary bifurcation
$s_1^{\mu=1/2}$	$0.128903 \pm 2 \times 10^{-7}$	double period bifurcation point
$s_1^{\mu=0}$	$0.138753 \pm 4 \times 10^{-7}$	coperiodic, turning point of speed
$s_2^{\mu=1/2}$	$0.140487 \pm 9 \times 10^{-7}$	double period bifurcation point
$s_2^{\mu=0}$	$0.140920 \pm 1 \times 10^{-6}$	coperiodic, turning point of speed
$s_3^{\mu=1/2}$	$0.141032049 \pm 5 \times 10^{-9}$	double period bifurcation point
$s_3^{\mu=0}$	$0.141056063 \pm 5 \times 10^{-9}$	coperiodic, turning point of speed

Table 1: Steepness of waves at the first few turning points of speed and at the double-period bifurcations.

The Table 1 indicates that there is a double-period bifurcation point enclosed between each turning point of speed,

$$0 < s_1^{\mu=1/2} < s_1^{\mu=0} \quad \text{and} \quad s_1^{\mu=0} < s_2^{\mu=1/2} < s_2^{\mu=0} \quad \text{and} \quad s_2^{\mu=0} < s_3^{\mu=1/2} < s_3^{\mu=0}.$$

We conjecture that the same pattern extends to the limiting wave, and

$$s_k^{\mu=0} < s_{k+1}^{\mu=1/2} < s_{k+1}^{\mu=0} \quad \text{for all } k = 0, 1, 2, \dots \quad (44)$$

where we defined $s_0^{\mu=0} := 0$. Analogous result can be obtained for other values of μ .

We would also like to refer the reader to the recent work [27] that uses singular value decomposition (SVD) of the Jacobian to identify bifurcation points. In addition, the latter work offers a way to determine fully nonlinear quasiperiodic traveling waves with two quasiperiods, and allow finding of secondary bifurcations from these quasiperiodic branches. Significance of subharmonic bifurcation points was emphasized in [65] as a possible route to determining of solitary waves.

6.2 Numerical Method

We seek solution of the eigenvalue problem:

$$\hat{S}_1 f = \xi f, \quad (45)$$

where ξ is a real eigenvalue, and $f(u)$ is a 2π -periodic eigenfunction. The linear operator \hat{S}_1 is self-adjoint,

$$\left(f \cdot \hat{S}_1 g \right) = \int f \hat{S}_1 g \, du = \int g \hat{S}_1 f \, du = \left(\hat{S}_1 f \cdot g \right). \quad (46)$$

The eigenvalue problem can be written in terms of the auxiliary variable, q , using the auxiliary conformal map [19]:

$$\tan \frac{u}{2} = L \tan \frac{q}{2} \quad \text{and} \quad u_q = \frac{2L}{1 + L^2 - (1 - L^2) \cos q} = \frac{1}{q_u}, \quad (47)$$

where $0 < L \leq 1$ is a parameter controlling the distribution of grid points, and u_q and q_u are 2π -periodic functions defined at collocation points. In the q variable, the operator \hat{S}_1 is given by:

$$\hat{S}_1 f(q) = q_u \left[\left(c^2 \hat{k}_q - g u_q \right) f - g \left(y \hat{k}_q f + f \hat{k}_q y + \hat{k}_q (y f) \right) \right], \quad (48)$$

where \hat{k}_q has the Fourier multiplier $|k|$ in the q -variable, i.e. $\hat{k}_q (e^{ikq}) = |k| e^{ikq}$. It is convenient to introduce a self-adjoint operator \hat{A} ,

$$\hat{A} f(q) := \left(c^2 \hat{k}_q - g u_q \right) f - g \left(y \hat{k}_q f + f \hat{k}_q y + \hat{k}_q (y f) \right), \quad (49)$$

so the eigenvalue problem may be written as follows:

$$\left[\hat{A} - \xi u_q \right] f(q) = 0, \quad \text{or} \quad \left[q_u^{1/2} \hat{A} q_u^{1/2} - \xi \right] h(q) = 0 \quad (50)$$

here $h(q) = u_q^{1/2} f(q)$. The first form is a generalized eigenvalue problem with a hermitian pair of operators (u_q is symmetric positive definite), or a regular eigenvalue problem with hermitian operator $q_u^{1/2} \hat{A} q_u^{1/2}$. The shift-inverse method (see also Ref. [66]) allows to determine the eigenvalue nearest to an arbitrary point σ in the spectral plane. It amounts to solving a sequence of linear problems given by

$$\left[q_u^{1/2} \hat{A} q_u^{1/2} - (\xi + \sigma) \right] f^{(n+1)} = f^{(n)}, \quad (51)$$

where σ is the shift, and superscript denotes the iteration number. The linear system (51) is solved by means of the minimal residual method (MINRES), and defines,

$$f^{(n+1)} = B_\sigma f^{(n)} \quad \text{where} \quad B_\sigma = \left[q_u^{1/2} \hat{A} q_u^{1/2} - (\xi + \sigma) \right]^{-1}. \quad (52)$$

The result, $f^{(n+1)}$ is a new basis vector for a subsequent Krylov subspace $\mathcal{K}_n(B_\sigma, f^{(0)}) = \text{span}\{f^{(0)}, B_\sigma f^{(0)}, \dots, B_\sigma^{n-1} f^{(0)}\}$. In the limit $n \rightarrow \infty$, the sequence of $f^{(n)}$ converges to the desired eigenfunction. The choice of the initial guess $f^{(0)}$ and the shift σ is made via the continuation method from the linear waves.

Advanced numerical methods (see Refs. [67, 68, 69]) are also available to seek multiple eigenvalues simultaneously. Note, that the operator matrix for B_σ is never formed, and applying the linear operator in (51) to an arbitrary 2π -periodic function via FFT is spectrally accurate and requires $O(mN \log N)$ flops, where m is the number of MINRES iterations that it takes to solve the associated linear system to a given tolerance. We considered up to 4×1024^2 Fourier modes and uniform grid to seek double period eigenfunctions using FFH method, and up to 16384 Fourier modes with nonuniform grid with $L \sim 0.005$.

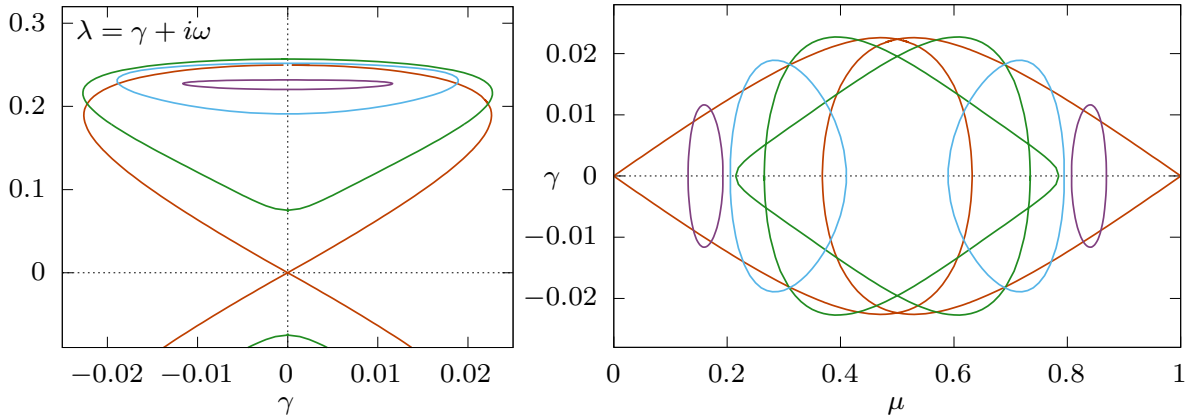


Figure 4: (Left Panel) The spectral plane showing BF instability in four Stokes waves with steepnesses $s = 0.095493$ (red), $s = 0.111408$ (green), $s = 0.119366$ (blue), and $s = 0.127324$ (violet). (Right Panel) The values of Floquet parameter μ vs real parts of eigenvalues γ for the BF instabilities only.

7 Results: Stability problem

In this section we illustrate the FFH method with canonical conformal variables based approach [59] in a sequence of simulations and determine the stability spectrum of Stokes waves for quasi-periodic perturbations. The Stokes waves themselves are computed by means of the Newton method coupled with the conjugate residual method [70, 71]. The library containing the Stokes waves is available at stokeswave.org and a discussion on how to compute Stokes waves can be found in Refs. [18, 19, 20].

7.1 Benjamin-Feir Instability

The Benjamin-Feir (BF), or modulational instability is dominant for Stokes waves with steepness less than $s \approx 0.12894$. It has been well-studied, and has a rigorous theoretical description in small amplitude waves regime [43]. In [41, 42] an asymptotic theory is developed giving excellent quantitative predictions for up to $s \approx 0.32$ ($ka \approx 0.1$). However, the BF instability for larger amplitude waves becomes challenging to study numerically since it is only present in a narrow band of the Floquet parameter μ . For example, in the work [59] $n = 64$ subharmonics were considered to study Benjamin-Feir instability in Stokes waves up to $s = 0.12732395$ ($ka = 0.4$). It was found that no Benjamin-Feir instability is present for $s = 0.12732395$ with $n = 64$ subharmonics. However, the FFH approach allows to scan arbitrary fine bands in Floquet parameter, and we demonstrate that BF instability persists for the wave with $s = 0.12732395$ albeit in a very narrow band in μ (see the violet curve in the Fig. 4).

In the left panel of Fig. 4 we show the spectrum of BF instability as steepness of Stokes wave increases, and the range of μ values is presented in the right panel. We find that the remnant of BF instability becomes qualitatively similar to the high-frequency instability as the figure-eight splits and shrinks.

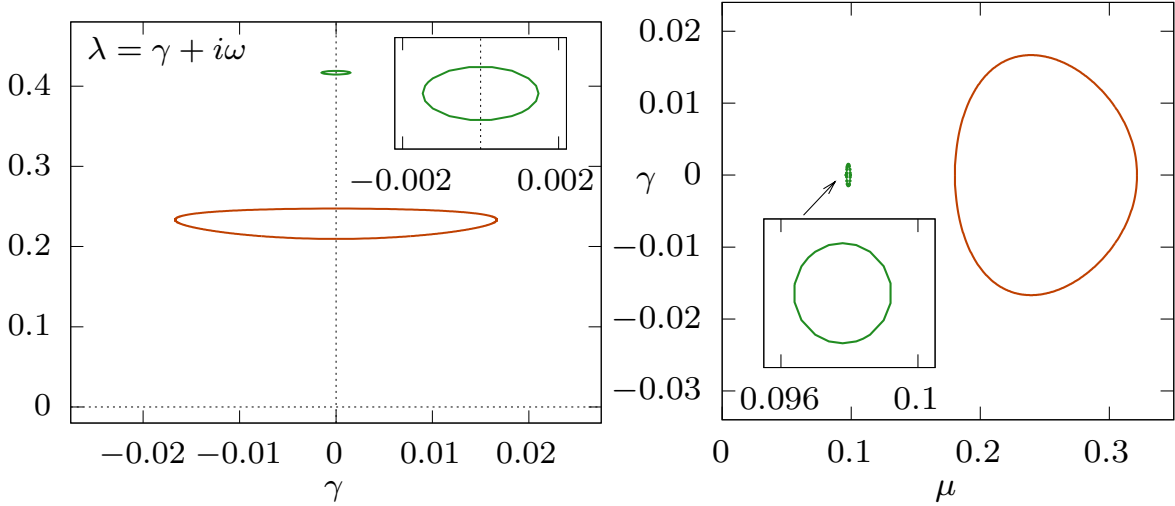


Figure 5: (Left Panel) The eigenvalues of (54) for the remnant of BF instability (orange) and the high-frequency instability (green) in a Stokes wave with $s = 0.1222625$, and (Right Panel) the growth rate, γ as a function of the Floquet parameter, μ , high-frequency instability is contained in the range $\mu \in (0.964, 0.992)$.

7.2 High-Frequency Instability

The high-frequency instability discovered in [44] is nontrivial to find because of the very limited range of the Floquet parameter, μ , for which it is present. In the left panel of Fig. 5 we show the spectral plane ($\lambda = \gamma + i\omega$) for $s = 0.1222625$ with the BF (red points) and the high-frequency instability (green points). The range of μ values vs growth rate, γ , of eigenvalues for BF and high-frequency instabilities is shown in the right panel. When compared to the remnant of the BF instability in Fig. 5, the range of Floquet multipliers for resolving the high-frequency instability is even finer. For example, for a Stokes wave with $s = 0.1222625$ the entire instability bubble is contained within the interval $\mu \in (0.964, 0.992)$ and would take a prohibitively large number of subharmonics unless FFH method is used. We observe that the growth rate for high-frequency instability can be significant, e.g for $s = 0.122262$ it reaches up to $\gamma = 1.48 \times 10^{-3}$ (see the Fig. 5).

7.3 Localized Instability

The localized instability branch appears before the first extremum of the Hamiltonian, and fully detaches at its extremum [47]. The localized branch dominates dynamics of steep waves, and induces wave-breaking in the nonlinear stage of time evolution of Stokes waves [35, 59]. In Fig. 6 we explore the spectrum of dynamical system for the Stokes wave with $s = 0.1366051511$. We found that the FFH method in canonical conformal variables is capable of extending the results of the numerical simulations in [59, 54]. It allows us to recover a continuous curve of eigenvalues, $\lambda(\mu)$, that corresponds to the localized instability branch [47].

We observe that the Floquet parameter has to be varied on a logarithmic scale around $\mu = 0$, so that the points on the $\lambda(\mu)$ curve are uniformly resolved in the vicinity of the point of superharmonic instability. We find that the results obtained

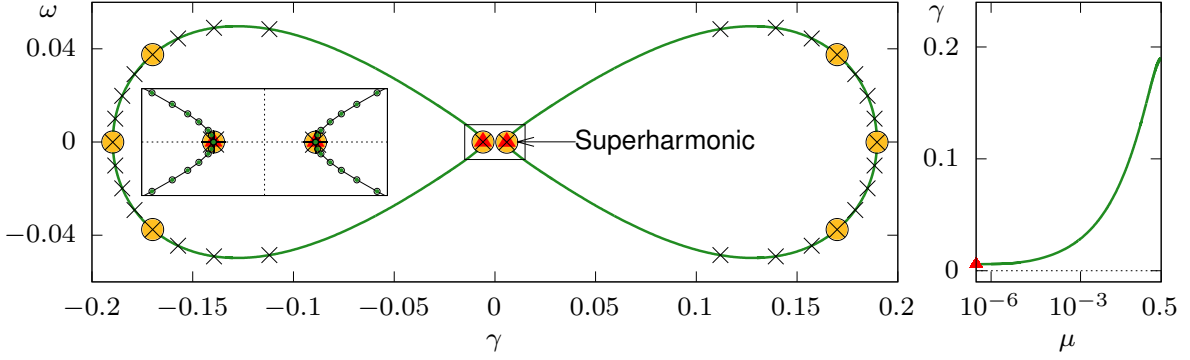


Figure 6: (Left Panel) Emergence of the localized instability in [47] for Stokes wave with steepness $s = 0.13660515$. Eigenvalues presented are found by three methods: the canonical conformal variables-based method (CCVM) with FFH (solid green, green circles in inset); CCVM from [59] with 1 (red triangles), 4 (gold circles) and 16 subharmonics (black crosses); matrix-forming linearization from [54] (black plus signs). (Right Panel) Growth rate as a function of μ for $\mu \in [0, 0.5]$ only positive values are shown.

with FFH approach together with canonical conformal variables based method are in agreement with the findings in [59, 54].

7.4 Numerical Method

The QEP is obtained by substitution $\partial_t \rightarrow \lambda$ into (31), and is given by:

$$\left[\lambda^2 \hat{\Omega}_{21}^\dagger \hat{k}^{-1} \hat{\Omega}_{21} - 2c\lambda \hat{H} - \hat{S}_1 \right] \delta y = 0, \quad (53)$$

where $\lambda = \gamma + i\omega$ is the eigenvalue that determines stability of the Stokes wave. The quasiperiodic case amounts to putting the subscript μ onto the respective operators:

$$\left[\lambda^2 \hat{\Omega}_{21,\mu}^\dagger \hat{k}_\mu^{-1} \hat{\Omega}_{21,\mu} - 2c\lambda \hat{H}_\mu - \hat{S}_{1,\mu} \right] p(u) = 0, \quad (54)$$

where we note that $\hat{\Omega}_{21,\mu}^\dagger \hat{k}_\mu^{-1} \hat{\Omega}_{21,\mu}$, $\hat{S}_{1,\mu}$ are self-adjoint operators and \hat{H}_μ is skew-adjoint. One can show that the dispersion relation for linear waves is,

$$\omega_\mu(k) = c(k + \mu) \pm \sqrt{g|k + \mu|}. \quad (55)$$

For numerical purposes it is more convenient to work with the first order system, given by:

$$\hat{k}_\mu \delta \phi = \lambda \hat{\Omega}_{21,\mu} \delta y \quad (56)$$

$$\hat{S}_{1,\mu} \delta y = \lambda \hat{\Omega}_{21,\mu}^\dagger \delta \phi - 2c\lambda \hat{H}_\mu \delta y, \quad (57)$$

or written in the block operator form:

$$\left(\hat{M}_\mu - \lambda \hat{L}_\mu \right) \begin{bmatrix} \delta \phi \\ \delta y \end{bmatrix} = 0, \quad (58)$$

and we proceed following the result in [59] to form the eigenvalue problem, however we include the FFH method [56]. We write the inverse operator to \hat{L}_μ as follows:

$$\hat{L}_\mu = \left[\begin{array}{c|c} 0 & \hat{\Omega}_{21,\mu} \\ \hline \hat{\Omega}_{21,\mu}^\dagger & -2c\hat{H}_\mu \end{array} \right] \text{ and } \hat{L}_\mu^{-1} = \left[\begin{array}{c|c} 2c\hat{R}_{12,\mu}^\dagger \hat{H}_\mu \hat{R}_{12,\mu} & \hat{R}_{12,\mu}^\dagger \\ \hline \hat{R}_{12,\mu} & 0 \end{array} \right], \quad (59)$$

and note that $\hat{L}_\mu^{-1} = \hat{R}_\mu^\dagger J_\mu^{-1} \hat{R}_\mu$, where we defined the operators from (28) with Floquet multiplier μ . We introduce the change of basis matrix \hat{R}_μ and the vector of canonical coordinates, $\mathbf{w} = (\delta\mathcal{P}, \delta y)^T = \hat{\Omega}_{21}^\dagger \mathbf{v}$, satisfying $\mathbf{w} = \hat{R}_\mu^\dagger \mathbf{v}$ where $\mathbf{v} = (\delta\phi, \delta y)^T$, by the relations:

$$\hat{R}_\mu = \hat{\Omega}_{\mu}^{-1} = \text{diag} \left(\hat{R}_{12,\mu} 1 \right), \quad \text{and} \quad \hat{R}_\mu^{-1} = \hat{\Omega}_\mu = \text{diag} \left(\hat{\Omega}_{21,\mu}, 1 \right), \quad (60)$$

and

$$\hat{J}_\mu = \left[\begin{array}{c|c} 0 & 1 \\ \hline 1 & -2c\hat{H}_\mu \end{array} \right]. \quad (61)$$

We write the shift–invert eigenvalue problem for the linearization on canonical coordinates \mathbf{w} with purely imaginary shift $i\sigma$ as follows:

$$\left(\hat{R}_\mu \hat{M}_\mu \hat{R}_\mu^\dagger - i\sigma J_\mu \right)^{-1} \hat{J}_\mu \mathbf{w} = \frac{1}{\lambda - i\sigma} \mathbf{w}. \quad (62)$$

The inverse operator in the left hand side is applied to an arbitrary 2π -periodic function via the formula:

$$\left(\hat{R}_\mu \hat{M}_\mu \hat{R}_\mu^\dagger - i\sigma J_\mu \right)^{-1} \begin{bmatrix} f \\ g \end{bmatrix} = \begin{bmatrix} \hat{Q}_\mu f \\ 0 \end{bmatrix} + \begin{bmatrix} i\sigma \hat{Q}_\mu \\ 1 \end{bmatrix} \hat{S}_{2,\mu}^{-1} \left(g + i\sigma \hat{Q}_\mu f \right). \quad (63)$$

Here $\hat{Q}_\mu := \hat{\Omega}_{21,\mu}^\dagger \hat{k}_\mu^{-1} \hat{\Omega}_{21,\mu}$ and $\hat{S}_{2,\mu} := \hat{S}_{1,\mu} + 2i\sigma \hat{H}_\mu + \sigma^2 \hat{Q}_\mu$ are applied in $O(N \log N)$ flops. The inverse to $\hat{S}_{2,\mu}$ is found from the solution of the linear operator equation by using the minimal residual (MINRES) method [66] with a diagonal preconditioner in Fourier space. Applying the inverse requires $O(mN \log N)$ flops, where $m \ll N$ is the number of iterations in MINRES.

8 Conclusions

We considered two eigenvalue problems that are fundamental to the study of Stokes waves and their stability. Numerical schemes are developed that allow to solve them efficiently via a matrix-free pseudospectral method with $O(N \log N)$ numerical complexity and suitable for the study of quasiperiodic eigenfunctions.

The first eigenvalue problem that we considered is posed for the linearization of the Babenko equation. The eigenfunctions of the linearized Babenko operator can be classified in two types – even and odd. Both types of eigenfunctions originate from $\cos(kx)$ and $\sin(kx)$ in a flat surface associated with a double eigenvalue (except for the $k = 0$ case). In a finite amplitude Stokes wave, the double eigenvalue breaks into a pair

of simple eigenvalues. Each one is associated with an even and an odd eigenfunction (shown in the left and right panels of Figs. 2–3). For all waves, zero is an eigenvalue associated with an odd eigenfunction, y_u , which is the derivative of the Stokes wave solution. In the waves at bifurcation points of \hat{S}_1 , the zero eigenvalue has double multiplicity and corresponds to one of the eigenvalues cross zero. Only eigenvalues associated with even eigenfunctions cross zero. The bifurcations occur at Stokes waves either at a turning-point in the speed (for co-periodic eigenfunctions), or at a secondary bifurcation to quasiperiodic branch (e.g. period doubling).

The second eigenvalue problem that was considered is posed for the linearization of the dynamical equations around a Stokes wave and governs its stability. It is shown how the stability problem can be interpreted as a second order pseudo-differential PDE and solved numerically by means of canonical conformal variables method [59] with the extension to quasiperiodic disturbances via the FFH approach [56]. We considered stability spectrum for waves studied in previous Refs. [54, 59] with the FFH approach and have shown accuracy and performance of the new method. We extended the results of the aforementioned works and reported novel physically relevant findings in the Ref. [47]. Additional results for dynamical spectrum in the vicinity of the limiting wave for the Benjamin-Feir, localized and high-frequency branches are a subject of ongoing research.

9 Acknowledgements

We would like to thank Eleanor Byrnes, Prof. Thomas Bridges, Prof. Bernard Deconinck, Prof. Alexander Korotkevich and Prof. Pavel Lushnikov for fruitful discussion and valuable suggestions. S.D would like to thank the Newton Institute at Cambridge University for hospitality during the “Dispersive hydrodynamics: mathematics, simulation and experiments” program. S.D. thanks the Department of Applied Mathematics at the U. of Washington for hospitality. A.S and S.D. acknowledge the FFTW project and its authors [72] as well as the entire GNU Project. A.S. thanks the Institute for Computational and Experimental Research in Mathematics, Providence, RI, being resident during the “Hamiltonian Methods in Dispersive and Wave Evolution Equations” program supported by NSF-DMS-1929284.

References

- [1] J. W. Miles, On the generation of surface waves by shear flows, *Journal of Fluid Mechanics* 3 (2) (1957) 185–204.
- [2] O. M. Phillips, On the generation of waves by turbulent wind, *Journal of fluid mechanics* 2 (5) (1957) 417–445.
- [3] H. Jeffreys, On the formation of water waves by wind, *Proceedings of the royal society of London. Series A, containing papers of a mathematical and physical character* 107 (742) (1925) 189–206.
- [4] G. G. Stokes, On the theory of oscillatory waves, *Transactions of the Cambridge Philosophical Society* 8 (1847) 441.

- [5] G. G. Stokes, Supplement to a paper on the Theory of Oscillatory Waves, *Mathematical and Physical Papers* 1 (1880) 314.
- [6] J. H. Michell, XLIV. The highest waves in water, *The London, Edinburgh, and Dublin Philosophical Magazine and Journal of Science* 36 (222) (1893) 430–437.
- [7] A. I. Nekrasov, On waves of permanent type I, *Izv. Ivanovo-Voznesensk. Polite. Inst.* 3 (1921) 52–65.
- [8] L. W. Schwartz, Computer extension and analytic continuation of Stokes’ expansion for gravity waves, *Journal of Fluid Mechanics* 62 (3) (1974) 553–578.
- [9] M. A. Grant, The singularity at the crest of a finite amplitude progressive Stokes wave, *J. Fluid Mech* 59 (part 2) (1973) 257–262.
- [10] J. M. Williams, Limiting gravity waves in water of finite depth, *Philosophical Transactions of the Royal Society of London. Series A, Mathematical and Physical Sciences* 302 (1466) (1981) 139–188.
- [11] J. M. Williams, *Tables of progressive gravity waves*, Boston : Pitman Advanced Pub. Program, 1985.
- [12] M. S. Longuet-Higgins, M. J. H. Fox, Theory of the almost-highest wave. Part 2. Matching and analytic extension, *J. Fluid Mech.* 85 (1978) 769–786.
- [13] M. Longuet-Higgins, M. Fox, Theory of the almost-highest wave: the inner solution, *Journal of Fluid Mechanics* 80 (4) (1977) 721–741.
- [14] S. J. Cowley, G. R. Baker, S. Tanveer, On the formation of moore curvature singularities in vortex sheets, *Journal of Fluid Mechanics* 378 (1999) 233–267.
- [15] M. S. Longuet-Higgins, On an approximation to the limiting stokes wave in deep water, *Wave Motion* 45 (6) (2008) 770–775.
- [16] G. Chandler, I. Graham, The computation of water waves modelled by nekrasov’s equation, *SIAM journal on numerical analysis* 30 (4) (1993) 1041–1065.
- [17] D. V. Maklakov, Almost-highest gravity waves on water of finite depth, *European Journal of Applied Mathematics* 13 (1) (2002) 67.
- [18] S. A. Dyachenko, P. M. Lushnikov, A. O. Korotkevich, Complex singularity of a Stokes wave, *JETP letters* 98 (11) (2014) 675–679.
- [19] P. M. Lushnikov, S. A. Dyachenko, D. A. Silantyev, New conformal mapping for adaptive resolving of the complex singularities of Stokes wave, *Proceedings of the Royal Society A: Mathematical, Physical and Engineering Sciences* 473 (2202) (2017) 20170198.
- [20] S. A. Dyachenko, V. M. Hur, D. A. Silantyev, Almost extreme waves, *arXiv preprint arXiv:2211.02875* (2022).

- [21] J. F. Toland, On the existence of a wave of greatest height and Stokes's conjecture, *Proceedings of the Royal Society of London. A. Mathematical and Physical Sciences* 363 (1715) (1978) 469–485.
- [22] C. J. Amick, L. E. Fraenkel, J. F. Toland, On the Stokes conjecture for the wave of extreme form, *Acta Mathematica* 148 (1) (1982) 193–214.
- [23] P. I. Plotnikov, A proof of the Stokes conjecture in the theory of surface waves, *Studies in Applied Mathematics* 108 (2) (2002) 217–244.
- [24] B. Chen, P. Saffman, Numerical evidence for the existence of new types of gravity waves of permanent form on deep water, *Studies in Applied Mathematics* 62 (1) (1980) 1–21.
- [25] J. A. Zufiria, Non-symmetric gravity waves on water of infinite depth, *Journal of Fluid Mechanics* 181 (1987) 17–39.
- [26] J. Wilkening, X. Zhao, Spatially quasi-periodic water waves of infinite depth, *Journal of Nonlinear Science* 31 (3) (2021) 1–43.
- [27] J. Wilkening, X. Zhao, Spatially quasi-periodic bifurcations from periodic traveling water waves and a method for detecting bifurcations using signed singular values, *Journal of Computational Physics* 478 (2023) 111954. doi:<https://doi.org/10.1016/j.jcp.2023.111954>.
- [28] V. E. Zakharov, Stability of periodic waves of finite amplitude on the surface of a deep fluid, *Journal of Applied Mechanics and Technical Physics* 9 (2) (1968) 190–194.
- [29] L. V. Ovsyannikov, *Dynamika sploshnoi sredy*, Lavrentiev Institute of Hydrodynamics, Sib. Branch Acad. Sci. USSR 15 (1973) 104.
- [30] S. Tanveer, Singularities in water waves and Rayleigh–Taylor instability, *Proceedings of the Royal Society of London. Series A: Mathematical and Physical Sciences* 435 (1893) (1991) 137–158.
- [31] S. Tanveer, Singularities in the classical Rayleigh–Taylor flow: formation and subsequent motion, *Proceedings of the Royal Society of London. Series A: Mathematical and Physical Sciences* 441 (1913) (1993) 501–525.
- [32] V. E. Zakharov, E. A. Kuznetsov, A. I. Dyachenko, Dynamics of free surface of an ideal fluid without gravity and surface tension, *Fizika Plasmy* 22 (1996) 916–928.
- [33] A. I. Dyachenko, V. E. Zakharov, E. A. Kuznetsov, Nonlinear dynamics of the free surface of an ideal fluid, *Plasma Physics Reports* 22 (10) (1996) 829–840.
- [34] G. R. Baker, C. Xie, Singularities in the complex physical plane for deep water waves, *Journal of fluid mechanics* 685 (2011) 83–116.
- [35] S. Dyachenko, A. C. Newell, Whitecapping, *Studies in Applied Mathematics* 137 (2) (2016) 199–213.

- [36] T. B. Benjamin, J. E. Feir, The disintegration of wave trains on deep water, *J. Fluid mech* 27 (3) (1967) 417–430.
- [37] T. Bridges, A. Mielke, A proof of the benjamin-feir instability, *Archive for rational mechanics and analysis* 133 (1995) 145–198.
- [38] M. J. Lighthill, Contributions to the theory of waves in non-linear dispersive systems, *IMA Journal of Applied Mathematics* 1 (3) (1965) 269–306.
- [39] G. B. Whitham, Non-linear dispersion of water waves, *Journal of Fluid Mechanics* 27 (2) (1967) 399–412.
- [40] V. E. Zakharov, L. A. Ostrovsky, Modulation instability: the beginning, *Phys. D* 540–548 (2009) 238.
- [41] M. Berti, A. Maspero, P. Ventura, Full description of Benjamin-Feir instability of Stokes waves in deep water, *Inventiones mathematicae* 230 (2) (2022) 651–711.
- [42] R. P. Creedon, B. Deconinck, A High-Order Asymptotic Analysis of the Benjamin-Feir Instability Spectrum in Arbitrary Depth, *Journal of Fluid Mechanics* 956 (20223) A29.
- [43] H. Q. Nguyen, W. A. Strauss, Proof of Modulational Instability of Stokes Waves in Deep Water, *Communications on Pure and Applied Mathematics* 76 (5) (2023) 1035–1084.
- [44] B. Deconinck, K. Oliveras, The instability of periodic surface gravity waves, *Journal of fluid mechanics* 675 (2011) 141–167.
- [45] A. S. Dosaev, Y. I. Troitskaya, M. I. Shishina, Simulation of surface gravity waves in the Dyachenko variables on the free boundary of flow with constant vorticity, *Fluid Dynamics* 52 (1) (2017) 58–70.
- [46] S. Murashige, W. Choi, Stability analysis of deep-water waves on a linear shear current using unsteady conformal mapping, *Journal of Fluid Mechanics* 885 (2020).
- [47] B. Deconinck, S. A. Dyachenko, P. M. Lushnikov, A. Semenova, The instability of near-extreme Stokes waves, *arXiv preprint arXiv:2211.05473* (2022).
- [48] T. B. Benjamin, Instability of periodic wavetrains in nonlinear dispersive systems, *Proceedings of the Royal Society of London. Series A. Mathematical and Physical Sciences* 299 (1456) (1967) 59–76.
- [49] R. P. Creedon, B. Deconinck, O. Trichtchenko, High-frequency instabilities of Stokes waves, *Journal of Fluid Mechanics* 937 (2022).
- [50] R. P. Creedon, A Complete Asymptotic Analysis of the Spectral Instabilities of Small-Amplitude Periodic Water Waves, *Ph.D. thesis* (2022).
- [51] M. S. Longuet-Higgins, The instabilities of gravity waves of finite amplitude in deep water I. Superharmonics, *Proceedings of the Royal Society of London. A. Mathematical and Physical Sciences* 360 (1703) (1978) 471–488.

- [52] M. Tanaka, The stability of steep gravity waves, *Journal of the physical society of Japan* 52 (9) (1983) 3047–3055.
- [53] M. Longuet-Higgins, M. Tanaka, On the crest instabilities of steep surface waves, *Journal of Fluid Mechanics* 336 (1997) 51–68.
- [54] A. O. Korotkevich, P. M. Lushnikov, A. Semenova, S. A. Dyachenko, Superharmonic instability of stokes waves, *Studies in Applied Mathematics* 150 (1) (2023) 119–134.
- [55] K. I. Babenko, Some remarks on the theory of surface waves of finite amplitude, in: *Doklady Akademii Nauk*, Vol. 294, Russian Academy of Sciences, 1987, pp. 1033–1037.
- [56] B. Deconinck, J. N. Kutz, Computing spectra of linear operators using the floquet–fourier–hill method, *Journal of Computational Physics* 219 (1) (2006) 296–321.
- [57] S. A. Dyachenko, P. M. Lushnikov, N. Vladimirova, Logarithmic scaling of the collapse in the critical keller–segel equation, *Nonlinearity* 26 (11) (2013) 3011.
- [58] P. M. Lushnikov, S. A. Dyachenko, N. Vladimirova, Beyond leading-order logarithmic scaling in the catastrophic self-focusing of a laser beam in kerr media, *Physical Review A* 88 (1) (2013) 013845.
- [59] S. A. Dyachenko, A. Semenova, Canonical conformal variables based method for stability of Stokes waves, *Studies in Applied Mathematics* 150 (3) (2023) 705–715. doi:<https://doi.org/10.1111/sapm.12554>.
- [60] Dyachenko, A. I. and Kuznetsov, E. A. and Spector, M. D. and Zakharov, V. E., Analytical description of the free surface dynamics of an ideal fluid (canonical formalism and conformal mapping), *Physics Letters A* 221 (1-2) (1996) 73–79.
- [61] A. I. Dyachenko, Y. V. Lvov, V. E. Zakharov, Five-wave interaction on the surface of deep fluid, *Physica D* 87 (1995) 233–261.
- [62] Dyachenko, A. I. and Lushnikov, P. M. and Zakharov, V. E., Non-canonical Hamiltonian structure and Poisson bracket for two-dimensional hydrodynamics with free surface, *Journal of Fluid Mechanics* 869 (2019) 526–552. doi:[10.1017/jfm.2019.219](https://doi.org/10.1017/jfm.2019.219).
- [63] J.-M. Vanden-Broeck, Some new gravity waves in water of finite depth, *The Physics of fluids* 26 (9) (1983) 2385–2387.
- [64] M. Longuet-Higgins, Bifurcation in gravity waves, *Journal of Fluid Mechanics* 151 (1985) 457–475.
- [65] J.-M. Vanden-Broeck, On periodic and solitary pure gravity waves in water of infinite depth, *Journal of Engineering Mathematics* 84 (1) (2014) 173–180.
- [66] Y. Saad, *Numerical methods for large eigenvalue problems*, Manchester University Press, 1992.

- [67] R. Lehoucq, D. Sorensen, C. Yang, Arpack users' guide: Solution of large scale eigenvalue problems with implicitly restarted Arnoldi methods, 1997, Available from netlib@ornl.gov under the directory scalapack (1989).
- [68] R. Lehoucq, K. Maschhoff, D. Sorensen, C. Yang, ARPACK software package, Rice University (1996).
- [69] G. W. Stewart, A krylov-schur algorithm for large eigenproblems, SIAM Journal on Matrix Analysis and Applications 23 (3) (2002) 601-614.
- [70] J. Yang, Newton-conjugate-gradient methods for solitary wave computations, Journal of Computational Physics 228 (18) (2009) 7007-7024.
- [71] J. Yang, Nonlinear waves in integrable and nonintegrable systems, SIAM, 2010.
- [72] M. Frigo, S. G. Johnson, The design and implementation of fftw3, Proceedings of the IEEE 93 (2) (2005) 216-231.